NaDES as a green technological approach for the solubility improvement of BCS class II APIs: An insight into the molecular interactions

Beatrice Albertini [a,*], Serena Bertoni [a], Stefano Sangiorgi [a], Giorgia Nucci [a], Nadia Passerini [a], Elisabetta Mezzina [b]

[a] Department of Pharmacy and BioTechnology, University of Bologna, Via S. Donato 19/2, 40127 Bologna, Italy
[b] Department of Chemistry "G. Ciamician", University of Bologna, Via San Giacomo 11, 40126 Bologna, Italy

ARTICLE INFO

ABSTRACT

Recently, Natural Deep Eutectic Solvents (NaDES) have emerged as potential solvents for boosting drug bioavailability. In this work, the mechanism of solubility enhancement of some APIs belonging to BCS class II (tolbutamide, nimesulide, domperidone and cinnarizine) in these eutectic bio-solvents was investigated in order to get deeper insights into the molecular interactions between the NaDES components and the selected drugs. Different NaDES formulations based on choline chloride, proline, solid organic acids (citric, tartaric and malic acid), sugars (glucose and xylitol) and water were prepared by mild heating (70 °C). Characterization of unloaded NaDES (pH, Karl Fisher titration, viscosity and FTIR analysis) indicated that the type of Hydrogen Bond Acceptor (HBA) and Hydrogen Bond Donor (HBD), their molar ratio as well as water amount strongly affect the extent of H-bonding interactions. Hard gelatin capsules filled with NaDES maintained their integrity until 6 months, proving that all water molecules participate in H-bond network. APIs' solubility enhancement was significant in all NaDES with respect to buffer solutions (pH 1.2 and 6.8). Analysing NaDES having Choline as HBA, it was found that the solubility of smaller molecules increased using larger HBD, while higher molecular weight APIs can be better inserted into the network formed by smaller HBD. NOE experiments demonstrated the formation of a robust supramolecular structure among the protons of choline, those of organic acid and water. In addition, 1D ROESY spectra revealed for the first time the crucial role of choline (methyl groups) in establishing hydrophobic interactions with the relative aliphatic or aromatic portion of the drugs. These data suggest the complex structure of the API-NaDES supramolecular assembly and underline that drug solubility is dependent on a balance network of H-bonds and hydrophobic interactions as well. Understanding the type of interactions between the API and NaDES is essential for their use as effective solubilisation aid.

1. Introduction

Nowadays the development of new formulation strategies for increasing the bioavailability of poorly water-soluble APIs is still a primary goal in the pharmaceutical technology field. Orally administered drugs, especially those belonging to BCS class II and IV, including new drug candidates, often require a challenging formulation design and suitable processing technologies to improve their limited solubility and/or dissolution behaviour (Göke et al., 2018). The pursued strategies are many and include, for example, crystal size reduction through several downstream processes as dry or wet milling, as well as bottom-up technologies as spray drying technique to obtain micronized powders, nanocrystals or nanosuspensions (Merisko-Liversidge and Liversidge, 2011)(Arora et al., 2018; Davis and Walker, 2018). Solubility improvement by solid-state properties modification aims to obtain amorphous drug dispersions (Bhujbal et al., 2021), co-crystals or polymorphs by means of enabling technologies based on either mechanical (Hasa et al., 2015; Zanolla et al., 2018) and thermal aids (Bertoni et al., 2019) or on solvent evaporation such as spray drying or freeze drying (Davis and Walker, 2018). Other strategies include complexation and the development of lipid-based micro/nano systems (Göke et al., 2018; Patel et al., 2018). All these approaches display pros and cons; the major issues are generally related to chemical and physical stability, limited drug loading, numerous manufacturing steps which also involve solvents, high production costs and low batch-to-batch reproducibility.

In the last decade, a great deal of attention has been addressed on

more sustainable pharmaceutical manufacturing processes. Some of the above-mentioned technologies are solvent free processes endorsing one principle of green chemistry (Bertoni et al., 2022, 2021). Beside these strategies, neoteric solvents, like Deep Eutectic Solvents (DES), represent an alternative approach for boosting drugs bioavailability (Álvarez and Zhang, 2019). DES are eutectic mixture obtained by the complexation of at least one Hydrogen Bond Acceptor (HBA) with a Hydrogen Bond Donor (HBD). The charge delocalization occurring through hydrogen bonding is responsible for the deep melting point depression of the mixture relative to the melting points of the individual components (Wang et al., 2019). These solvents display several interesting properties, such as non-flammability, low-vapour pressure, ease of preparation, tunability and high biocompatibility (Zhao et al., 2015). Hence, they have been exploited in different fields of chemistry (Smith et al., 2014)(i.e., extractions, organic synthesis, biochemistry, biocatalysis) up to the most recent application in the pharmaceutical formulations (Hansen et al., 2021; Mokhtarpour et al., 2020; Zainal-Abidin et al., 2019).

More recently, Natural DES (NaDES) have been evaluated for the solubility and bioavailability enhancement of some poorly water-soluble substances (Dai et al., 2013; Liu et al., 2018), among various applications. In particular, NaDES are binary or ternary systems constituted by nontoxic substances naturally occurring in food and plants, such as choline derivatives, sugars, amino acids and organic acids mixed in a proper molar ratio. NaDES have attracted the attention of the scientific community due to their sustainable properties. In fact, they can be prepared by mild heating and gentle stirring and their components are abundantly present in nature, readily available and biorenewable (Mišan et al., 2020).

Several papers have investigated the suitable combinations, preparation method and physicochemical properties of these bio-based solvents (Dai et al., 2013; Sut et al., 2017). All the analysed NaDES displayed strong intermolecular interactions via hydrogen bonding, mainly dependent on the nature and amount of the neat components, including water, often added to reduce both temperature and preparation time as well as the viscosity at RT (Craveiro et al., 2016; Savi et al., 2019). The usual HBA are quaternary ammonium salts (e.g. choline chloride) or amino acids (e.g. betaine, proline and glycine), while HBD are sugars (e.g. sucrose, glucose, fructose among others) or organic acid (mainly citric, tartaric and malic acids). Acids, amino acids and alcohols may also behave as HBA. The number of their possible arrangements is impressive and they might be designed as tailor-made solvents, according to their intended application (Mišan et al., 2020). Until now, the selection and the combination between HBA and HBD has been mainly based on a trial and error approach observing the formation of a clear solution and its stability over time (Dai et al., 2013). Recently, several studies have applied computational methods to better understand the properties of the hydrogen bonded networks of NaDES (Hansen et al., 2021).

Focusing on the solubilizing ability of NaDES, different combinations of choline chloride, amino acids, sugars and organic acids have been tested on several molecules and macromolecules. First, Dai and co-workers (Dai et al., 2013) demonstrated that the solubility of rutin, quercitin and cinnamic acid significantly increased in choline chloride and glucose-based NaDES compared to water. Faggian and co-workers enhanced the oral bioavailability of rutin in rats using a proline:glutamic acid (1:1) eutectic mixture (Faggian et al., 2016). Similarly, the bioavailability of berberine was increased up to 8 times administering to mice a NaDES composed of proline, malic acid, lactic acid and water (1:0.2:0.3:0.5) with respect to the water suspension (Sut et al., 2017). Oliveras et al (Olivares et al., 2018) formulated a betaine and urea (1:1.5) NaDES with a 2 % w/w water added to stabilize β-lactam antibiotics without affecting their antimicrobial activity. Further, the enhancement of lidocaine solubilisation into different arginine based-NaDES with several organic acids was attributed to the H-bonding between the DES components and the drug (Gutiérrez et al., 2019). More

recently, the solubility of several drugs has been tested in a series of NaDES with different composition, specifically choline chloride or betaine-based, organic acid-based and sugar based and compared to the corresponding solubility in neat solvents (acetic acid, lactic acid and propylene glycol) (Mustafa et al., 2021). The authors observed an improvement of the drug solubility in the tested NaDES, hypothesizing the formation of a hydrogen bonds network between the NaDES and the drug molecules. In particular, the greater solubility of trimethoprim and methylphenidate in acidic NaDES has been related to bonds involving the amino groups of drugs. In the case of spironolactone, griseofulvin and nitrofurantoin the authors supposed that ketone groups in drug structures may act as electron pair donors towards carboxyl moieties of acids. The results suggested that, albeit with a different extent, the drugs might have become part of a new supramolecular assembly based on H-bonding and composed on NaDES components, the drug itself and water. In this vein, a study was carried out to understand the nature of intermolecular interactions of choline-based DES and several hydrophobic drugs (LogP 0.5–3.4) (Mokhtarpour et al., 2020). Since all the investigated drugs have the ability to act as HBD or HBA, the authors stated that drugs having carboxyl and/or hydroxyl groups could interact with the –OH, C=O and Cl moieties of DES via H bonds. However, despite these considerations, further research are necessary to better investigate the mechanisms of dissolution enhancement in these eutectic biosolvents (Liu et al., 2022).

The aim of this study was to get deeper insights into the molecular interactions between NaDES and APIs with low water solubility. NaDES with different composition were characterized in terms of pH, viscosity, water content and solubilizing ability towards different poorly water soluble drugs belonging to BCS class II (drugs with low solubility and high permeability). Specifically, four APIs, cinnarizine (CIN), tolbutamide (TBM), nimesulide (NIM) and domperidone (DOM) were selected for their different physicochemical characteristics, such as log P, pKa, solubility in physiological buffers and melting point, as reported in Table 1. The molecular interactions between drug and NaDES were analysed by FTIR and NMR spectroscopy.

2. Experimental

2.1. Materials

Choline chloride (purity ≥ 98 %, MW = 139.62 g/mol), D-(+)-glucose (≥99.5 %, MW = 180.156 g/mol), L-(-)-malic acid (≥95 %, MW = 134.0874 g/mol), L-proline (≥99 %, MW = 115.13 g/mol), xylitol (≥99 %, MW = 152.15 g/mol) and sucrose (≥99.5 %, MW = 342.3 g/mol) were purchased from Sigma Aldrich (Steinheim, Germany). Citric acid (≥99 %, MW = 192.124 g/mol) was bought from Carlo Erba (Milan, Italy). DL-Tartaric acid (≥99 %, MW = 150.087 g/mol) was obtained from Fluka (Steinheim, Germany). The APIs Cinnarizine, Nimesulide and Tolbutamide were purchased from Sigma Aldrich. Domperidone was bought from A.C.E.F. S.p.A (PC, Italy). The characteristics of the selected APIs are reported in Table 1.
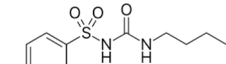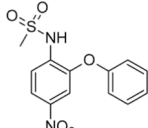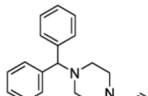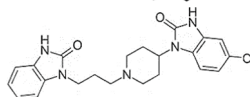
Gelatin capsules type "0″ (having a capacity of 0.68 mL) were provided by Fagron (BO, Italy). For Karl Fisher titration Aquagent® Solvent and Aquagent® Titrant 5 (Scharlab, Barcelona, Spain) were used.

All other chemicals used for HPLSW analysis were of analytical grade.
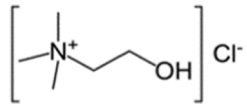
2.2. Preparation of NaDES
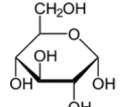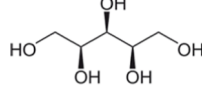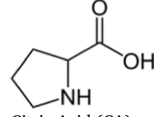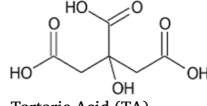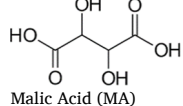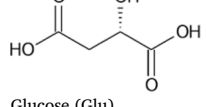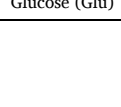
NaDES with a specific molar ratio were prepared in glass scintillation vials with caps by stirring the mixture of solids slowly setting the temperature at 70 °C until a clear and homogeneous solution was observed. A certain amount of water was included in NaDES composition. Specifically, increasing amounts of water in 2.5 % w/w aliquots were added during preparation in order to allow NaDES formation and/or to reduce the preparation time and viscosity. Finally, the mixture was allowed to

Table 1
structure and characteristics of BCS class II APIs under investigation and experimental solubility data measured at 25 °C.

APIs	Chemical structure	MW (g/mol)	pKa	Log P	MP (°C)	Water solubility (μg/mL)	Solubility (μg/mL) pH 1.2	pH 6.8
TBM		270.35	5.16[a]	2.34[a]	128.5	109 (37 °C)[a]	106.98 ± 17.96	897.87 ± 49.42
NIM		308.31	6.7[b]	2.56[b]	143–144.5	18.2[b]	6.95 ± 0.02	10.88 ± 0.00
CIN		368.52	8.1[c]	5.77[c]	117–121	750[c]	3281.58 ± 406.74	0.75 ± 0.30
DOM		425.91	7.9[d]	9.90[d]	242.5	0.986[d]	221.92 ± 6.67	10.28 ± 0.00

([c] Https://go.drugbank.com/drugs/DB00568, n.d.; [a] Https://go.drugbank.com/drugs/DB01124, n.d.; [d] Https://go.drugbank.com/drugs/DB01184, n.d.; [b] Https://go.drugbank.com/drugs/DB04743, n.d.).

Table 2
Composition of the NaDES prepared by heating at 70 °C and their corresponding processing time.

NaDES	HBA	HBD	Molar ratio	Added H$_2$O (% w/w)	Time(h)
1	Choline Chloride (Ch Cl)	Glucose (Glu)	5:2	2.5	3
2		Xylitol (Xyl)	5:2	5	2.5
3		Proline (Pro)	2:1	27.5	0.5
4		Citric Acid (CA)	3:1	7.5	1
5			2:1	7.5	0.5
6		Tartaric Acid (TA)	2:1	7.5	0.5
7		Malic Acid (MA)	1:1	5	0.5
8	Proline (Pro)	Glucose (Glu)	1:1	22.5	2
9		Xylitol (Xyl)	1:1	20	1
10	Citric Acid (CA)	Glucose (Glu)	1:1	20	1.5

cool down to RT. The final composition of prepared NaDES is reported in Table 2.

2.3. Characterization of NaDES

The final **water content** of the studied samples was calculated by Karl-Fisher titration (SI Analytics® TitroLine® 7500 KF, Scharlab, Barcelona Spain). At least six runs for each NaDES were performed. The **pH** of the diluted NaDES was measured using a pH-meter (pH 80, XS Instruments, MO, Italy). The **density** of the NaDES was assessed by a simple gravimetric procedure, using a calibrated volume (10–500 µl) at RT.

The **viscosity** of NaDES was measured using a viscosimeter Visco Star R (Fungilab SA, Barcelona, Spain), setting at 25 °C the temperature of sample adapter of the rheometer. Based on the initial screening, the measuring element spindle number TR8 was selected and rotated at 12 rpm. Three different samples for each NaDES composition were prepared and measurements were carried out in duplicate on each sample. The viscosity values were expressed in mPa·s. The viscosity was also measured after the addition of increasing amount (1 % w/w) of water until a very low degree of dilution.

2.4. Solubility measurements

Solubility measurements of APIs (CIN, TBM, NIM and DOM) were performed at 25° C. For the solubility assessment in water-based solutions, an excess of each API was added to 10 mL of the respective medium (buffer solutions at pH 1.2 and 6.8). The samples were magnetically stirred for 48 h and the suspensions were then twice centrifuged at 10.000 rpm for 10 min. The supernatants were suitably diluted with water before the analysis and detected by UV–Visible spectrometer (Cary 60, Agilent Technologies GmbH, Waldbronn, Germany). Each sample was analysed at least in triplicate.

The conditions used for the quantification of the APIs were the following: CIN was detected at 253 nm using a linearity curve in the range of 5–60 µg/mL ($R^2 = 0.9999$, 1 mg/ml stock solution in ethanol properly diluted with a HCl 0.1 M); TBM was detected at 235 nm using a linearity curve in water in the range of 5–45 µg/mL ($R^2 = 0.9998$, 1 mg/ml stock solution in ethanol properly diluted with water); NIM was analysed at 301 nm using a linearity curve in the range of 5–30 µg/mL ($R^2 = 0.9984$, 1 mg/ml stock solution in ethanol properly diluted with water); while DOM was detected at 284 nm using a linearity curve in the range of 1–20 µg/mL ($R^2 = 0.99941$, 1 mg/ml stock solution in ethanol properly diluted with a HCl 0.1 M solution).

The solubility of the APIs in the prepared NaDES was evaluated adding an excess of each drug into 1 mL of NaDES contained in a 2 mL Eppendorf. The samples were magnetically stirred for 48 h and the suspensions were then threefold centrifuged (Eppendorf Centrifugate 5810R) at 14.000 rpm for 10 min. The supernatants were suitably diluted with the proper solvent (as above indicated) and analysed spectroscopically. Each sample was analysed at least in triplicate.

Statistical analysis was performed with one-way analysis of variance (ANOVA) followed by the Bonferroni posthoc test (GraphPadPrism, GraphPad software, Inc., San Diego, CA, USA).

2.5. FT-IR analysis

Fourier Transform-Infrared Spectra (FT-IR) Analysis of neat HBA and HBD substances, NaDES (3–10), raw drugs and drug-loaded NaDES were carried out with an IR spectrophotometer (Jasco FT-IR A-200, Pfungstadt, Germany), using the KBr disc method. The scanning range was 650–4000 cm^{-1} and the resolution was 1 cm^{-1}. The samples were mixed with KBr and compressed into a tablet (about 10 mm in diameter and 1 mm in thickness), using a hydraulic press (Perkin Elmer, Beaconsfield, UK), at 3 tons, for 3 min.

2.6. NMR measurements

NMR experiments were performed on some NaDES samples using a Varian Inova spectrometer (14.1 T 51-mm Bore Oxford Superconducting Magnet equipped with a triple-resonance PFG indirect probe and a SW-PFG Probe) operating at 600 MHz, and the acquisitions were carried out at 25 °C, 50 °C and 80 °C. The solutions were transferred into 5-mm NMR tubes equipped with coaxial capillary tube containing D_2O. The external deuterated solvent provided both lock frequency and ^1H spectrum reference [δ_{HDO} = 4.76 ppm (25 °C); 4.51 ppm (50 °C) 4.21 ppm (80 °C)].

2D NOESY (Nuclear Overhauser Enhancement SpectroscopY) experiments were carried out at 50 °C in phase sensitive mode employing 90° angle pulse of 8.3 ms, a spectral width of 15 ppm in each dimension, 64 t1 increments, 8 scans for each increment, delay 1.5 s, and mixing time 300–800 ms.

1D ROESY (Rotating Frame Overhauser Enhancement SpectroscopY) experiments were measured at 50 °C and 80 °C using 90° angle pulses optimized for each temperature with a spectral width of 12 ppm delay 1.5 s, and mixing time 50–200 ms. Selective pulses width of 50 Hz and spin lock power of 2 KHz were employed.

3. Results and discussion

3.1. NaDES production and characterization

NaDES differing in terms of chemical composition (choline chloride-based; proline-based and citric acid-based, Table 2) were firstly prepared by selecting the HBA:HBD molar ratio from literature (Dai et al., 2013; Shafie et al., 2019; Sut et al., 2017). We excluded liquid-based components (e.g. lactic acid or glycerol) for the NaDES preparation since they are usually excellent solvent themselves for many organic compounds. Then, a proper evaluation of the right amount of water to add to the eutectic mixture was carried out. In fact, water plays a key role in favouring the formation of H-bonds between the NaDES components, enabling the formation of a clear solution upon heating and even after cooling at RT (Dai et al., 2013). For example, NaDES 3, 8, 9 and 10 required at least 20 % w/w of water (Table 2) in order to obtain the formation of a clear solution at RT, whereas other NaDES could be formed also without water. However, the addition of water was important to decrease NaDES viscosity. In fact, depending on the water percentage, the viscosity of the eutectic solution significantly decreased influencing the solubilisation of active compounds (Dai et al., 2015). It is reported that a water amount up to 40 % w/w reduces the viscosity while keeping the supramolecular structure, as water molecules interact with both the HBA and HBD forming hydrogen bonds (Mustafa et al., 2021). Thus, in the case of NaDES with excessive viscosity (NaDES 1–2 and 4–7, Table 2), aliquots of 2.5 % w/w of water were added to mixtures until reaching a homogeneous fluid with an acceptable viscosity to allow handling, stirring or other practical activities. NaDES were then prepared adding all the water at once: as expected, at higher water amount the preparation time shortened and ranged between 30 min and 3 h (Table 2). The results evidence that choline-based solvents required lower amount of water for their formation than NaDES containing proline and citric acid as HBA. However, NaDES 1 and 2 resulted unstable during storage, suggesting that the selected molar ratio and/or the amount of added water was not appropriate. In particular, NaDES 2 started the crystallization process after 12 h, while NaDES 1 recrystallized after 6 days stored in the close bottle at RT.

The effective amount of water in stable NaDES (3–10) was analysed by Karl Fisher titration and the values are reported in Fig. 1. The results evidenced that water contents of the majority of NaDES were higher (differences ranging 1–4 %) than the theoretical ones, calculated on the amount of water added during preparation, probably due to the hygroscopicity of the neat compounds, especially of ChCl.

Hard gelatin capsules (type 0) were then filled by a syringe with two

A

NaDES	Calculated water amount (%) ± SD	pH	Viscosity ± SD (mPa·s)
3	31.36±1.33	7.0	40*/
4	8.56±0.10	2.0-2.5	2070±170
5	8.51±0.08	2.0-2.5	3327±340
6	8.11±0.08	1.5-2.0	2693±101
7	6.00±0.20	1.5-2.0	2115±304
8	24.61±0.17	6.0-6.5	2070±210
9	20.67±0.36	7.0	1008±238
10	20.50±0.45	1.0-1.5	3980±57

B

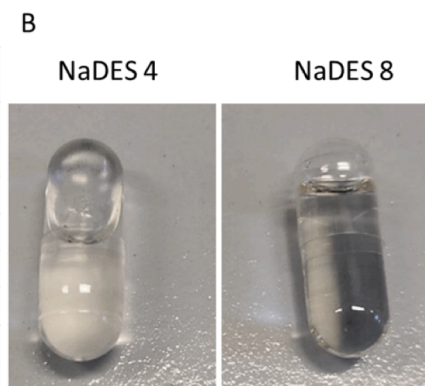*NaDES 4*   *NaDES 8*

*/ Out of instrumental range

Fig. 1. A) Characteristics of stable NaDES (n = 8); B) Gelatine type 0 capsules filled with NaDES 4 and 8 containing about 8.5 % and 25 % w/w of water, respectively.

NaDES samples (NaDES 4 and 8) containing different amount of water and wrapped by aluminium foil at RT during storage, as shown in Fig. 1 B. Weight and structural integrity of the capsules stored for at least 6 months were maintained for both NaDES, even for the one with high water content (NaDES 9). It appeared, thus, that there was no "free water", i.e. water molecules participating in the H-bonding network were not available to act as plasticizer/solvent towards the gelatine shell.

Another NaDES important parameter, especially when used to dissolve ionisable molecules, is pH. In this study TBM and NIM were selected as examples of weak acids, while CIN and DOM as examples of weak bases (Table 1). The specific pH values for each mixture are shown in Fig. 1. NADES were thus divided into two categories: acidic NaDES 4–7 and 10 (pH 1–3) and neutral NaDES 3, 8 and 9 (pH 6–7).

The viscosity of NaDES was measured at 25 °C and the results are reported in Fig. 1, while Fig. 2 shows the influence of further water addition to the NaDES samples. Apart from NaDES 3, all the other samples were quite viscous (1000–4000 mPa·s), including NaDES 8 and 10 containing more than 20 % w/w of water. Comparing NaDES 4 and 5, the viscosity increased with increasing the molar ratio of citric acid, as previously observed (Shafie et al., 2019).

Regardless the starting viscosity values, small addition of water caused a large decrease of viscosity in all samples. In particular, the viscosity of choline-based NaDES reduced by 32–36 % compared to the original value after addition of 1 % w/w water and decreased by 80–81 % when diluted with 5 % water. The viscosity decrease of the other samples (NaDES 8–10) was slightly lower: about 16–25 % and 57–71 % after 1 % and 5 % of water addition, respectively. After the addition of 10 % water the viscosity decreased by about 93 % of the original values for choline-based NaDEs and about 75–88 % for NaDES 8–10. A water surplus lead to an aqueous solution of the individual components with negligible chemical interactions (viscosity < 100 mPa·s), in agreement with what was observed in some choline chloride-based DES when water exceeded the 30 % w/w (Rozas et al., 2021). Despite the 20 % of added water during preparation, NaDES 10 showed the highest viscosity and an additional 22 % water was required to break the the NaDES supramolecular structure. Zhekenov and co-workers (Zhekenov et al., 2017) using molecular dynamics simulations demonstrated the reduction of H-bonds between HBA and HBD, while increased the H bonds with the neat components with water.

To better analyse the interactions between the components and the effect of water in NaDES interactions, FTIR studies were performed. Here the FTIR analysis of acidic-based eutectic mixtures are first described. Comparing the spectra of the single components with those of NaDES, vibrational shifts emerged at higher (redshift) and at lower (blueshift) frequencies indicating the formation of hydrogen bonds (Table 3). In particular, the FTIR spectrum of choline chloride depicts bands at 949 cm^{-1}, 1091 cm^{-1}, 1478 cm^{-1} and 3268 cm^{-1} which correspond respectively to N(CH$_3$)$_3$ bending, C—N stretching, CH$_3$ rocking vibration and O—H stretching. Organic acids display a band around 1700 cm^{-1} corresponding to the stretching of C=O, the OH stretching vibration around 3400 cm^{-1} and various bands between 1000 and 1200 cm^{-1} which would be correlated to the stretching of sp^2 and sp^3 C—O. The spectra of NaDES 4–7 (Figure S1) reveal a wide band between 2900 and 3700 cm^{-1} relative to O—H stretching. The shift of the OH stretching band (ν_{OH}) to higher wavenumbers for choline chloride and to lower frequencies for organic acids is very pronounced in NADES compared to single pure compounds, as reported in Table 3. This indicates a strong interaction, likely due to hydrogen bonds involving these groups (O—H on Choline to C=O; O—H on acid to Cl$^-$ etc.). The
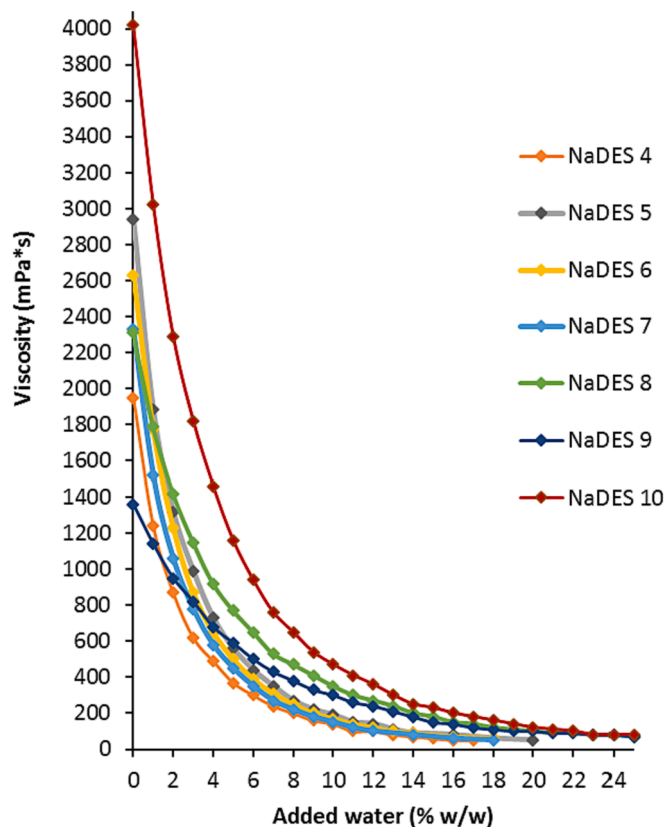

Fig. 2. Effect of dilution of stable NaDES containing different amount of starting water.

Table 3
FTIR vibrational shifts of the main groups of acidic NaDES compared to the neat components. Blue and red shift- values moved to higher or lower wavelength for more than 2 cm^{-2}, respectively.

Shifts (cm^{-1})		NaDES 4	NaDES 5	NaDES 6	NaDES 7	NaDES 10
ChCl						
N$^+$ (CH$_3$) bending	949.8	954.6	955.6	955.6	954.6	
C—N stretching	1091.5	1082.8	1081.9	1083.8	1105.0	
O—H stretching	3268.7	3357.5	3390.2	3365.2	3366.1	
Citric acid						
C=O	1742.4	1731.8	1730.8			1732.7
O—H stretching	3449.1	3357.5	3390.2			3419.2
Tartaric acid						
C=O	1740.4			1740.4		
O—H stretching	3405.7			3365.2		
Malic acid						
C=O	1714.4				1732.7	
O—H stretching	3392.2				3366.1	
Glucose						
O—H stretching	3397.0					3419.2

main difference between NaDES 4 and 5 (**Figure S1a, SI**) is the displacement of the OH stretching band, which is probably due to the different molar ratio between ChCl and citric acid, as the amount of added water is the same. Furthermore, shifts of the C—N stretching of choline and of the carboxylic group of organic acids are observed (Table 3). All these NADES exhibit a shift of N$^+$(CH$_3$)$_3$ group of choline at about 950 cm^{-1}, indicating a further interaction involving choline nitrogen. These findings are in agreement with previous studies, that showed clear shifts of the wavenumbers of the functional groups due to H-bond interactions between the DES components (Gautam et al., 2020; Olivares et al., 2018; Shafie et al., 2019). FTIR spectrum of NaDES 6 shows a lower displacement of the O—H of tartaric acid, while the frequency of C=O stretching (ν_{CO}) is unchanged (**Figure S1b, SI**). On the contrary, NaDES 7 displays clear shifts of both ν_{OH} and ν_{CO} (**Figure S1c, SI**). Finally, NaDES 10, composed by citric acid as HBA and glucose as HBD, shows displacements of both the carbonyl group of the acid (blueshift) and of the broad band at about 3400 cm^{-1} (**Figure S1d, SI**), supporting again the hydrogen bonding between the hydroxyl groups of glucose and CA. In addition, this NaDES contains a larger water amount (Table 3) compared to the other mixtures with acid character, suggesting the involvement of water in the H-bond network with CA and glucose.

Regarding NaDES 3, 8 and 9, the main vibrational shifts are reported in Table 4 and the FTIR spectra are depicted in **Figures S2, SI** (a, b and c, respectively). NaDES 3 displays vibrational shifts of choline Cl bands similar to previous NaDES, while only the ν_{OH} band of proline is shifted. Similarly, the analysis of NaDES 8 and 9 spectra reveals the blueshift of ν_{OH} in proline, while does not evidence shifts of the ν_{CO} stretching vibration band (Table 4). These results confirm the formation of hydrogen-bond network, within which water plays a pivotal role being $\geq$ 20 % w/w.

Table 4
FTIR vibrational shifts of the main groups of neutral NaDES compared to the neat components. Blue and red shift- values moved to higher or lower wavelength for more than 2 cm^{-2}, respectively.

Shifts (cm^{-1})		NaDES 3	NaDES 8	NaDES 9
ChCl				
N$^+$ (CH$_3$) bending	949.8	955.6		
C—N stretching	1091.5	1084.8		
O—H stretching	3268.8	3398.9		
Proline				
C=O	1623.8	1625.7	1621.8	1622.8
O—H stretching	3407.6	3398.9	3398.0	3387.4
Glucose				
O—H stretching	3397.0		3398.0	
Xylitol				
O—H stretching	3388.3			3387.4

Therefore, the investigated NaDES are ternary systems in which water (accounting for 6–8 % in acid NaDES and in the range 20–30 % for neutral ones) acts as a HBD, similarly to other polyols used in different DES formation (Wang et al., 2019). The very broad bands observed in the O—H stretching vibration region (2900–2700 cm-1) for the investigated NaDES may be attributed to the sum of several contributions of different type of hydroxyl groups forming the network of H-bonding in these samples, i.e. OH-groups of water, as well as those of organic acids and sugars.

3.2. Evaluation of APIs solubility in NaDES

First of all, the solubility of the selected APIs in water solutions at different pH was assessed and the results are reported in Table 1. TBM displays higher solubility (about 8 times) in phosphate buffer than in acidic pH but still<1 mg/mL. NIM solubility is very low (about 10 µg/mL) in both pH conditions. As for the bases, DOM solubility increased at pH 1.2, but the pH-sensitivity was even higher for CIN, which passes from a negligible solubility in phosphate buffer (<1µg/mL) to an equilibrium solubility of about 3 mg/mL in acidic pH.

Analysing first acidic NaDES as solubilizing vehicles (Fig. 3A), the solubility values for all drugs significantly increased, regardless of the acid-base character of the active molecule. In particular, TBM reached the highest solubility in NaDES 4 composed by choline chloride and citric acid (3:1 M ratio) going from 0.1 to about 7 mg/mL (67-fold increase). However, the value was not significantly different from that found for NaDES 5, indicating that the different molar ratio between choline chloride and citric acid was not discriminating in terms of TBM solubility enhancement. For all other drugs, NaDES 7 resulted the best solvent displaying a solubility enhancement of 243, 593 and 22 times for NIM, DOM and CIN, respectively.

The solubility values achieved in acidic NaDES were higher compared to those in neutral NaDES. This was not surprising for the two weak bases CIN and DOM. In particular, DOM displayed 553-fold increase in the eutectic composed by proline-glucose 1:1 and 22.5 % of water. The solubility of CIN was increased by 1300 times in NaDES 8 and NaDES 9 (Fig. 3B). Surprisingly, the higher solubilizing capacity of acidic NaDES over neutral ones was observed for TBM. In fact, the values of solubility increase for TBM in neutral NaDES were the lowest among all APIs. In this regards, it should be mentioned that TBM solubility in pH 6.8 phosphate buffer was considerably high (about 0.9 mg/ml) and therefore the order of magnitude of the solubility increase in neutral DES was modest. For NIM, only NaDES 8 allowed a considerable solubility enhancement, while the solubility values obtained in NaDES 3 and 9 were lower than the acidic NaDES.

Therefore, for three of the four analysed drugs, the best performances were displayed by acid NaDES 7 and neutral NaDES 8. These results
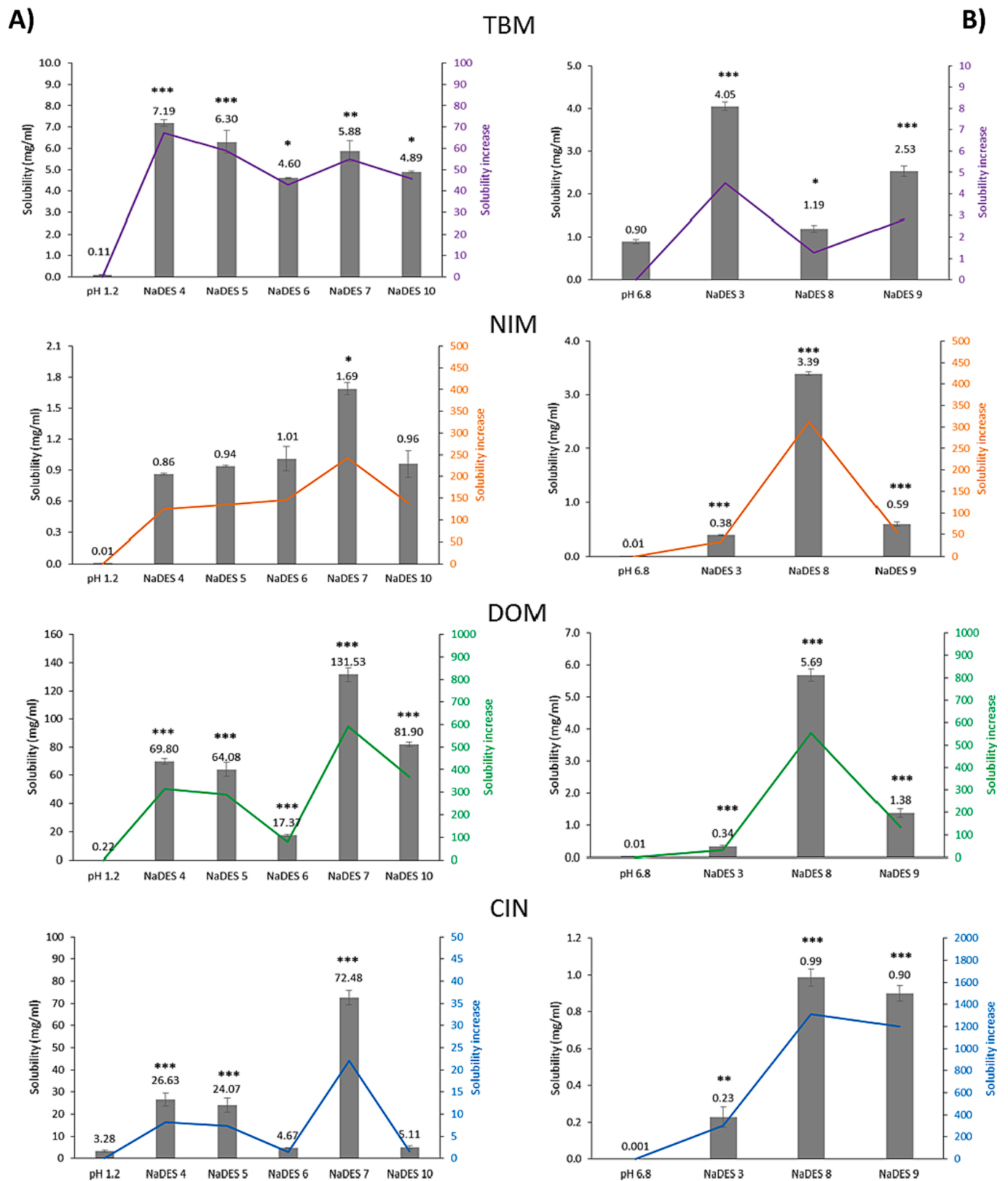
Fig. 3. Solubility values of the APIs in. a) acidic NaDES and b) neutral NaDES compared to the corresponding aqueous solution. Values are expressed as mean (n = 3) ± S.D. * p < 0.5, **p < 0.01 and ***p < 0.001, significant difference compared to the solubility in aqueous solution (pH 1.2 or 6.8).

suggest that the solubilization mechanism through a supramolecular assembly between DES components and water is prevalent on the pH-dependent drug solubilisation process. Among acidic solvents, NaDES 4, 5 and 7 resulted the best ones. In particular, NaDES 4 and 5 behaved

in the same way as solubilisation aid, while NaDES 7 acted distinctly. Their different solubilisation ability towards the analysed drugs suggests that the type of organic acid (CA has got three –COOH groups and one –OH group while MA has two carboxyl groups and one less –CH2) might

influence the network of interactions, but it could also be due to the different molar ratio between ChCl and the organic acid, specifically 3:1 for NaDES 4, 2:1 for NaDES 5 and 1:1 for NaDES 7, as well as to the different water amount (NADES 4 and 5 contain 2.5 % water more than NaDES 7). Moreover, it may be assumed that TBM, being a smaller molecule that the others (Table 1), can better interact with a larger HBD (CA), while DOM and CIN can be better inserted into the network formed by smaller HBD such as MA. Nevertheless, worthy of note is that NaDES 4 and 7 exhibit similar viscosity (around 2000 mPa·s, Table 3), suggesting similar extent of intermolecular interactions between NaDES components. Therefore, their solubilization ability towards the APIs may not only depend on H-bonds and the solubilized drug might be involved in the supramolecular assembly also through different interactions.

With regard to neutral NaDES, the eutectic mixture based on Pro, Glu and water (NaDES 8) is the most promising one, except for TBM that is better solubilized in NaDES 3. Both contain Pro, thus it can be hypothesized prevalent interactions between TBM and ChCl than between TBM and glucose. In addition, the type of sugar appeared to play an important role for the H-bond network: comparing NaDES 8 and 9 with TBM, the solubility increased with Xyl, while, for NIM and DOM, glucose accounted for the best performance. For CIN, there was no significant difference between the solubility obtained in these solvents.

Finally, comparing the solubility increases in all formulations, it seems that the amount of water cannot be considered a discriminating variable. As above described, solubility enhancement is mainly influenced by the type of HBA and HBD employed for NaDES preparation.

In order to better understand the solubilisation ability of the studied NaDES towards the selected APIs, an investigation into the molecular interactions was then performed.

3.3. Evaluation of chemical interactions in API-loaded NaDES

The FTIR spectra of drug-loaded NaDES depicted only the bands previously described for the eutectic mixtures making difficult the identification of the characteristic bands of the drugs. The results only showed slight shifts of the broad band at about 3300 cm^{-1}, suggesting the involvement of the APIs within the H-bond network. As an example,

the FTIR spectra of NaDES 5 containing the studied APIs is reported in **Figure S3 (SI)**.

Hence, NMR analysis was used to deeply investigate the interactions between the drugs reported in Table 1, and some acid/choline-based NaDES, *i.e.*, NaDES 4 and NaDES 7, containing citric acid (CA) and malic acid (MA), respectively.

The results obtained for neutral NaDES (3, 8 and 9) and NaDES 10 with high water amount are not reported because the aromatic signals of the drug were completely covered by the intense peaks of water and the signals of sugars and Pro are overlapped with a large area of aliphatic peaks.

3.3.1. TBM in NaDES 4

Spectra of pure NaDES 4 and of a solution of TBM in this eutectic mixture have been recorded at 25 °C and 50 °C. At both temperatures, chemical shifts of components of the eutectic did not change, but the resolution of signals improved dramatically with increased temperature. Therefore, NOE experiments aiming to provide information on intra and intermolecular interactions involving close protons in space concerning the eutectic components and TMB protons, were carried out at 50 °C.

In Fig. 4 1H NMR spectra of NaDES 4 (spectrum a) and of 0.022 M solution of TBM (spectrum b) are reported.

At 50 °C the spectrum of NaDES 4 shows sharp peaks of choline (*a,b,c* protons) and citric acid (*d*), while water and overlapped exchangeable OH display a broadened signal centred around 6.4 ppm. In trace b (Fig. 4) the spectrum of 22 mM TMB in NaDES 4 is displayed. Obviously, signals of the solute are visible increasing the intensity of all the signals considerably. In particular aromatic (*f,g*), methyl (*e*), and butyl (*i,l,m*) protons are detectable, while aliphatic CH$_2$ (*h*) signal falls under the peaks of ChCl resulting not visible.

NOE experiments have been acquired in order to get insights on the solution structures of the drug/NaDES 4 mixture. The presence of NOE crosspeaks between protons from different species indicates spatial contacts of < 5 Å. In particular, we used 2D NOESY technique to examine the interactions that may be associated to the formation of the liquid phase of NaDES 4. Fig. 5 shows a NOESY spectrum region at mixing time 300 ms; spectra at different times were also recorded (t$_{mix}$ = 100–500 ms). Already at 300 ms strong negative crosspeaks appeared
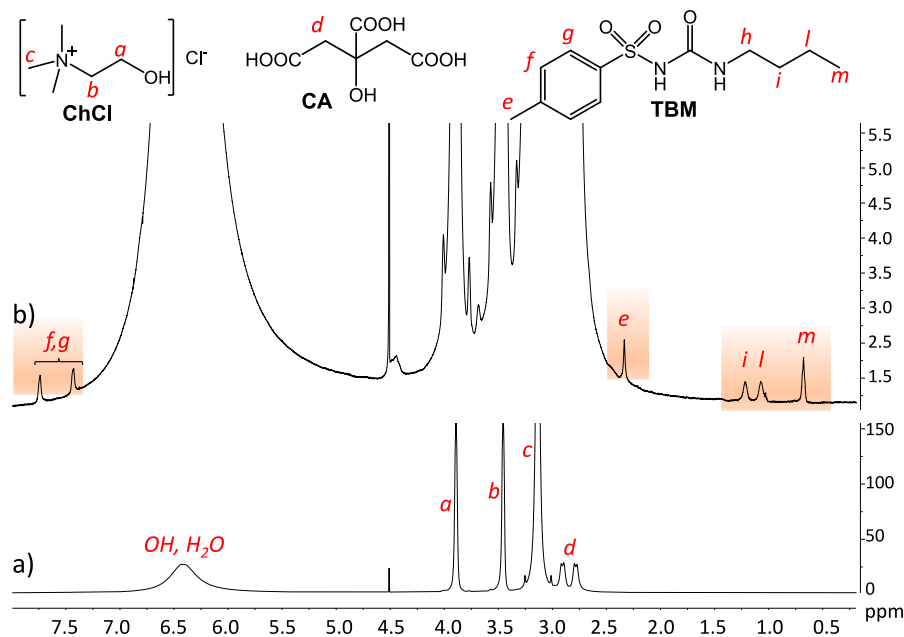

Fig. 4. ^{1}H NMR Spectra at 50 °C of a) NaDES 4 (ChCl/CA 3:1, 7.5 % H$_2$O); b) 22 mM TMB in NaDES 4 (orange box, peaks related to TBM). NaDES 4 and TBM signals are labelled using the letters reported in the above structures. (For interpretation of the references to colour in this figure legend, the reader is referred to the web version of this article.)
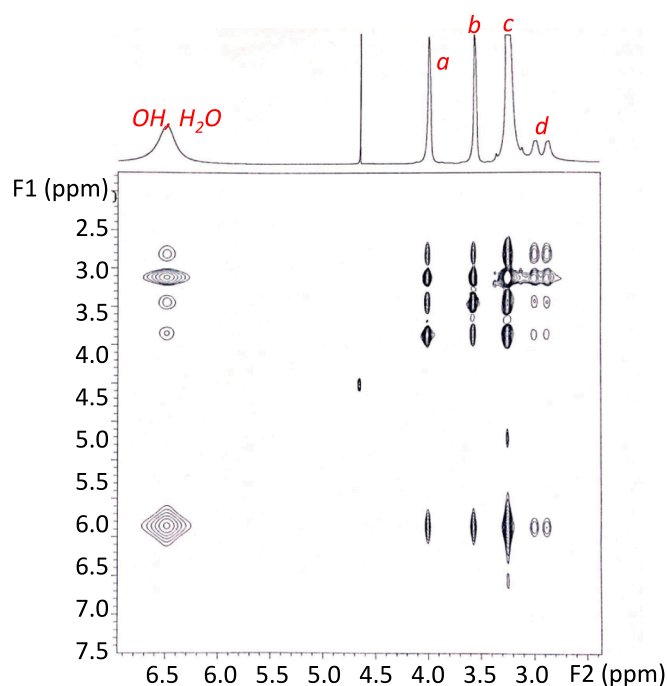
Fig. 5. Partial spectrum 2D NOESY at 50 °C of NaDES 4. Signals of NaDES 4 are labelled according to the letters reported on structures of ChCl and CA (eutectic components) in Fig. 4.

among all the proton signals (aliphatic and exchangeable hydrogens), evidencing the existence of interactions between the protons from the different species throughout space. It should be noted that all the cross-correlations involving aliphatic hydrogens and mobile protons are in phase with the diagonal, meaning that the correlation times (τ_c) of the corresponding molecules are typical of large structures ($\omega\tau_c \gg 1$). This is an indication that NaDES 4 mixture behaves as a supramolecular structure, according to data previously reported (Caprin et al., 2021; Delso et al., 2019; Zahrina et al., 2018). Strong NOE couplings between choline and CA, as well as choline or CA with water, respectively, suggest the formation of an extended and robust aggregated structure, presumably kept together by a network of H-bond, (Dai et al., 2013) in which also water might participate. The most intense interactions are displayed by the methyl groups of choline. However, in the case of water protons, whose broad peak at 6.4 ppm overlap the OH signals of choline

and CA, in principle, it is not possible to distinguish whether the detected correlations in these spectra are generated by NOE intra-molecular and/or intermolecular interactions.

NOESY spectra of a sample of 22 mM TMB in NaDES 4 were also registered at 50 °C. These spectra are superimposable to those registered previously in absence of TBM, in these experiments no cross peaks correlating protons of TBM with those of NaDES were revealed.

In order to detect a direct involvement between the eutectic components and the drug so highlighting the presence of specific aggregates (El Achkar et al., 2020; Park et al., 2020), a number of 1D ROESY spectra were acquired by applying selective pulses of 50 Hz on each signal of choline chloride and citric acid. Fig. 6 reports 1D ROESY spectrum of 22 mM TMB in NaDES 4 acquired employing a selective pulse on the resonance at 3.14 ppm corresponding to trimethylammonium protons $N^+(CH_3)_3$ of ChCl.

The spectrum shows a significant increase of signals corresponding to the butyl protons (*i,l,m*) of TBM, despite the limits of low signal/noise ratio due to the large difference of concentration between solute and eutectic solvent. In the same spectrum no peaks of aromatic protons of the drug (*f,g*) were detected. On the contrary 1D ROESY spectra (see Figure S4, SI) irradiating the other signals of the eutectic, i.e. choline or CA methylene protons (3.89/3.45 ppm and 2.78/2.90 ppm, respectively) and water broad signal, did not reveal increasing of TBM signals. In addition, all these ROE experiments show important intermolecular interactions among the protons of ChCl, those of citric acid and water/mobile hydrogens occurring in the eutectic itself, as previously observed in the NOESY spectra described above.

Summarizing, the whole data suggest a spatial involvement of the aliphatic region of the drug with the methyls of choline, indicating a predominant interaction of hydrophobic nature between the two moieties.

3.3.2. TBM in NaDES 7

NaDES 7 is a choline-based eutectic containing malic acid (MA) in 1:1 equimolar ratio. Water is present in the mixture (about 6 % w/w) and its broad signal includes also mobile protons of ChCl and MA. For the same reasons explained above, all spectra were recorded at 50 °C. Fig. 7 shows stacked spectra comparing neat eutectic (trace a), 18 mM TBM solution in NaDES 7 (spectrum b), and 1D ROESY of the same solution (trace c) obtained irradiating Ch trimethylammonium protons signal with a soft pulse.

Similarly, as in the case discussed before, also in these experiments the role of choline is crucial in establishing hydrophobic interactions with butyl group of TMB. Irradiation of methyls of ammonium ion
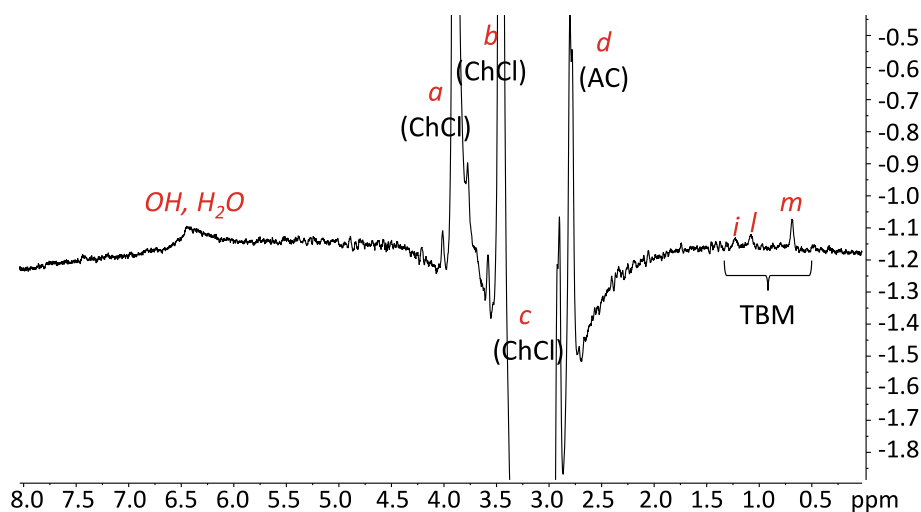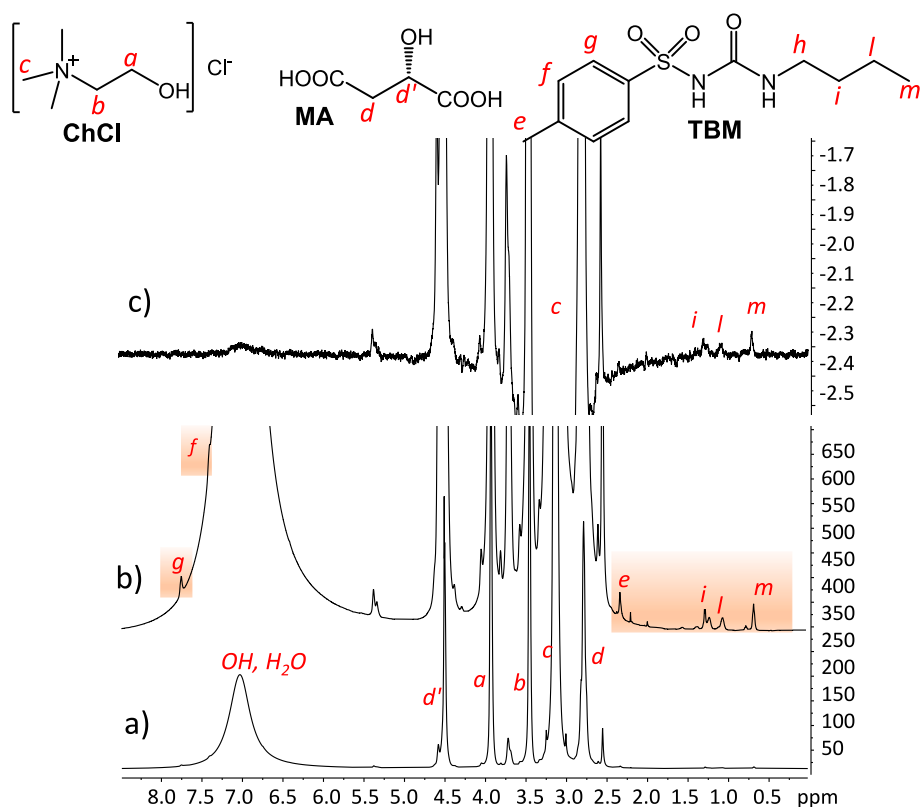

Fig. 6. 1D ROESY spectrum 22 mM TMB in NaDES 4 (t_{mix} 100 ms) at 50 °C. The spectrum was acquired selectively pulsing choline methyl protons $N^+(CH_3)_3$ (labelled with letter *c*). Positive ROE peaks relative to the butyl group of TBM (protons *i,l,m*) are clearly visible in the spectrum. See structures of Fig. 4 for the labels.

Fig. 7. ^{1}H NMR Spectra at 50 °C of a) NaDES 7 (ChCl/MA 1:1); b) 18 mM TMB in NaDES 7 (orange box, peaks related to TMB); c) 1D ROESY selectively irradiating choline methyl protons N[+](CH₃)₃ (labelled with letter *c*). Positive ROE peaks relative to the butyl group of TMB (protons *i,l,m*) are visible in the spectrum. NaDES 7 and TBM signals are labelled using the letters reported in the structures. (For interpretation of the references to colour in this figure legend, the reader is referred to the web version of this article.)

caused enhancements of signal protons *i, l,* and *m*, while phenyl protons peaks did not appear, as well as ROE enhancements were not detected after selective irradiation of the other signals of ChCl and those of malic acid.

3.3.3. DOM in NaDES 4

In order to get sharper signals in the ^{1}H spectrum of the solution of the drug in NaDES 4, we decided to increase temperature to 80 °C. Thereby some signals of DOM are not covered by the intense peaks of the eutectic resulting clearly visible. In particular, Fig. 8A show signals of
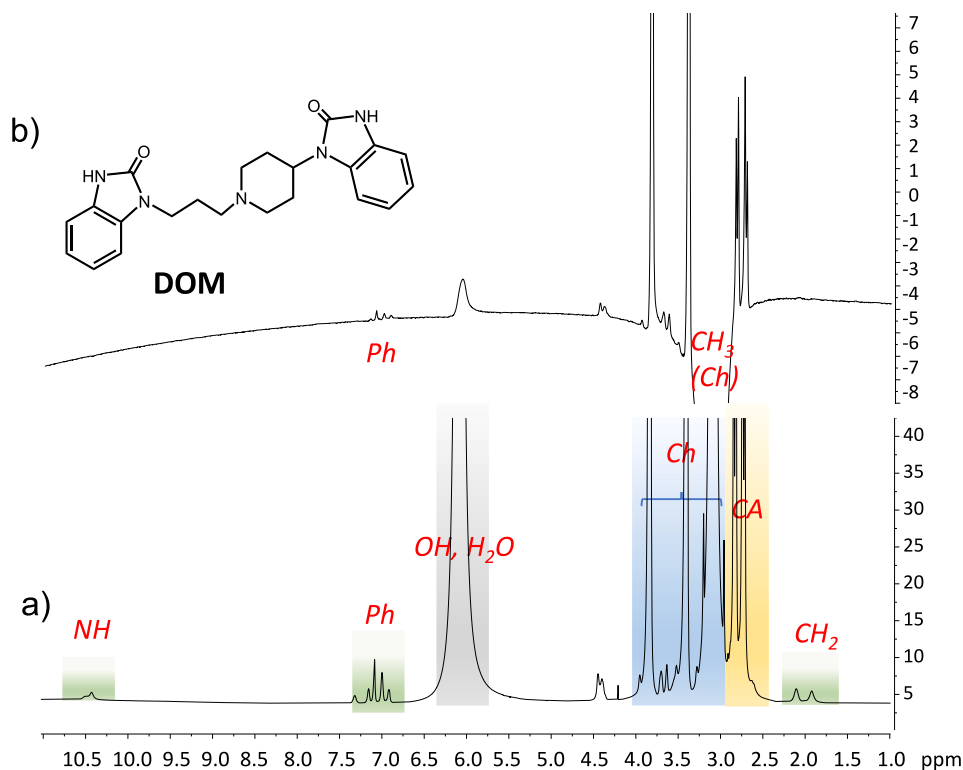
Fig. 8. a) ^{1}H NMR Spectrum at 80 °C of 0.12 M DOM in NaDES 4 (Grey box, peaks related to water/mobile protons; blue box, peaks related to choline chloride (ChCl); yellow box, peaks related to citric acid (CA) and green box, peaks related to DOM); b) 1D ROESY partial spectrum at 80 °C of 0.12 M DOM in NaDES 4 (t_{mix} 100 ms) obtained selectively irradiating choline methyl protons N[+](CH₃)₃. Positive ROE peaks relative to aromatic protons of DOM are detected. (For interpretation of the references to colour in this figure legend, the reader is referred to the web version of this article.)

N—H, aromatic and some aliphatic protons in the green box.

Acquisition of 1D ROESY spectrum irradiating choline trimethyl-lammonium moiety gave an interesting correlation with the aromatic protons of DOM (Fig. 8b), while the other peaks (NH, aliphatic) were not raised. Similar results were obtained studying the behaviour of the other signals of choline (protons *a* and *b*). The spectra (Figure S5, SI) show weaker ROE aromatic protons peaks than those observed in Fig. 8b. As in the case discussed above, perturbing CA protons did not produce any ROE enhancements of the proton peaks of DOM. Again the role of ChCl is important to establish specific aggregate formation with the solute, however in this case the interaction involves the aromatic portion of DOM, the analysis of the NMR results does not confirm if one or both phenyls correlate with choline of the eutectic.

3.3.4. DOM in NaDES 7

The behaviour of DOM in choline-based NaDES 7 eutectic solvent containing malic acid (MA) was not studied because the signals of the drug were completely covered by the intense peaks of the solvent at the range of temperatures investigated (25–90 °C).

3.3.5. CIN in NaDES 4 and 7

This drug possesses three aromatic rings that form the main portion of the molecule. We could observe the relative signals at 80 °C in a region of 3 mM spectrum of the drug in NaDES 4 that is free from eutectic signals. The results are comparable to those exposed in the case of DOM (Figures S6 and 7, SI). Again choline methyl ammonium protons caused enhancements of aromatic protons of CIN. However, it should be noted that the spectrum of the drug solution did not display other signals corresponding to aliphatic protons of CIN that are presumably overlapped with the eutectic signals, so that analysis of the actual interactions is not complete.

The analysis of CIN in NaDES 7 was not carried out owing to signal overlapping with the solvent protons.

3.3.6. NIM in NaDES 4 and 7

Unfortunately, all the signals of NIM fall under those of both components of the eutectic mixtures, and therefore it was not possible to study its behaviour and the relative structural interactions with the eutectic even by varying the temperature.

4. Conclusions

In this study, several NaDES formulations, containing mainly choline chloride as HBA and substances such as proline, organic acids and sugars acting as HBD, were used to enhance the solubilisation of poorly soluble APIs belonging to BCS class II. TBM and NIM were selected as examples of weak acids and CIN and DOM as weak bases. All the studied NaDES were ternary systems based on HBA, HBD and water. Some eutectic mixtures, mainly based on choline chloride and organic acids, formed also in absence of water dilution but low water additions (5–7.5 % w/w) were necessary to reduce their viscosity and to ameliorate their handling. Differently, the other NaDES required at least 20 % w/w of water for the formation of clear solutions. It is noteworthy that gelatin capsules filled with these solvents maintained their structural integrity for 6 months, confirming that there was not "free water" and all water molecules were included in the H-bonding network formed by HBA and HBD, as evidenced by FT-IR analysis. The results of solubility study highlighted the ability of these vehicles to increase the solubility of the low-water soluble APIs through the formation of a hydrogen-bonded supramolecular assembly. The different behaviour of NaDES towards the selected APIs was found to be mainly related to the type of HBD and HBA and to their different molar ratio rather than the pH of the eutectic mixture. In particular, acid NADES 4 and 7 (ChCl:CA and ChCl:MA at 3:1 and 1:1 M ratio, respectively) displayed the best performance. Surprisingly, NMR studies performed on some organic acid/choline-based NaDES (4 and 7) revealed the presence of hydrophobic interactions

between the methyl substituents of ammonium cation of ChCl and the butyl group of TBM, the aromatic portion of DOM, and the aliphatic protons of CIN, respectively. Until now, these interactions within the supramolecular assembly have never been reported in the literature.

Therefore, it can be concluded that the solubilisation mechanism of NaDES towards the poorly soluble drugs is quite complex and depends not only to the extent of intra/intermolecular H-bonds but even to hydrophobic interactions between drug and ChCl. These findings are important for better understanding the role of choline-based natural eutectic mixture as solubilisation enhancers. Ultimately, it has been demonstrated that these liquid systems can be used to develop a solid dosage forms by filling hard gelatine capsules.

CRediT authorship contribution statement

Beatrice Albertini: Conceptualization, Validation, Writing – original draft, Supervision. **Serena Bertoni:** Formal analysis, Writing – review & editing. **Stefano Sangiorgi:** Investigation, Data curation, Visualization. **Giorgia Nucci:** Investigation, Data curation. **Nadia Passerini:** Resources, Writing – review & editing. **Elisabetta Mezzina:** Investigation, Writing – original draft.

Data availability

Data will be made available on request.

Appendix A. Supplementary material

Supplementary data to this article can be found online at https://doi.org/10.1016/j.ijpharm.2023.122696.

References

Álvarez, M.S., Zhang, Y., 2019. Sketching neoteric solvents for boosting drugs bioavailability. J. Control. Release 311–312, 225–232. https://doi.org/10.1016/j.jconrel.2019.09.008.

Arora, D., Khurana, B., Rath, G., Nanda, S., Goyal, A.K., 2018. Recent advances in nanosuspension technology for drug delivery. Curr. Pharm. Des. 24, 2403–2415. https://doi.org/10.2174/1381612824666180522100251.

Bertoni, S., Albertini, B., Passerini, N., 2019. Spray congealing: an emerging technology to prepare solid dispersions with enhanced oral bioavailability of poorly water soluble drugs. Molecules 24, 3471. https://doi.org/10.3390/molecules24193471.

Bertoni, S., Albertini, B., Ronowicz-Pilarczyk, J., Calonghi, N., Passerini, N., 2021. Solvent-free fabrication of biphasic lipid-based microparticles with tunable structure. Pharmaceutics 14, 54. https://doi.org/10.3390/pharmaceutics14010054.

Bertoni, S., Hasa, D., Albertini, B., Perissutti, B., Grassi, M., Voinovich, D., Passerini, N., 2022. Better and greener: sustainable pharmaceutical manufacturing technologies for highly bioavailable solid dosage forms. Drug Deliv. Transl. Res. 12, 1843–1858. https://doi.org/10.1007/s13346-021-01101-6.

Bhujbal S. V, Mitra B, Jain U, Gong Y, Agrawal A, Karki S, Taylor L.S, Kumar S, (Tony) Zhou Q, 2021. Pharmaceutical amorphous solid dispersion: A review of manufacturing strategies. Acta Pharmaceutica Sinica B 11, 2505–2536. 10.1016/j.apsb.2021.05.014.

Caprin, B., Charton, V., Rodier, J.D., Vogelgesang, B., Charlot, A., Da Cruz-Boisson, F., Fleury, E., 2021. Scrutiny of the supramolecular structure of bio-sourced fructose/glycerol/water ternary mixtures: towards green low transition temperature mixtures. J. Mol. Liq. 337, 116428 https://doi.org/10.1016/j.molliq.2021.116428.

Craveiro, R., Aroso, I., Flammia, V., Carvalho, T., Viciosa, M.T., Dionísio, M., Barreiros, S., Reis, R.L., Duarte, A.R.C., Paiva, A., 2016. Properties and thermal behavior of natural deep eutectic solvents. J. Mol. Liq. 215, 534–540. https://doi.org/10.1016/j.molliq.2016.01.038.

Dai, Y., van Spronsen, J., Witkamp, G.-J., Verpoorte, R., Choi, Y.H., 2013. Natural deep eutectic solvents as new potential media for green technology. Anal. Chim. Acta 766, 61–68. https://doi.org/10.1016/j.aca.2012.12.019.

Dai, Y., Witkamp, G.-J., Verpoorte, R., Choi, Y.H., 2015. Tailoring properties of natural deep eutectic solvents with water to facilitate their applications. Food Chem. 187, 14–19. https://doi.org/10.1016/j.foodchem.2015.03.123.

Davis, M., Walker, G., 2018. Recent strategies in spray drying for the enhanced bioavailability of poorly water-soluble drugs. J. Control. Release 269, 110–127. https://doi.org/10.1016/j.jconrel.2017.11.005.

Https://go.drugbank.com/drugs/DB00568, n.d. No Title [WWW Document]. URL https://go.drugbank.com/drugs/DB00568 (accessed 7.27.22).

Https://go.drugbank.com/drugs/DB01124, n.d. No Title [WWW Document]. URL https://go.drugbank.com/drugs/DB01124 (accessed 7.27.22).

Https://go.drugbank.com/drugs/DB01184, n.d. No Title [WWW Document]. URL https://go.drugbank.com/drugs/DB01184 (accessed 7.27.22).

Https://go.drugbank.com/drugs/DB04743, n.d. No Title [WWW Document].

Delso, I., Lafuente, C., Muñoz-Embid, J., Artal, M., 2019. NMR study of choline chloride-based deep eutectic solvents. J. Mol. Liq. 290 https://doi.org/10.1016/j.molliq.2019.111236.

El Achkar, T., Moufawad, T., Ruellan, S., Landy, D., Greige-Gerges, H., Fourmentin, S., 2020. Cyclodextrins: from solute to solvent. Chem. Commun. 56, 3385–3388. https://doi.org/10.1039/d0cc00460j.

Faggian M, Sut S, Perissutti B, Baldan V, Grabnar I, Dall'Acqua S, 2016. Natural Deep Eutectic Solvents (NADES) as a tool for bioavailability improvement: Pharmacokinetics of rutin dissolved in proline/glycine after oral administration in rats: Possible application in nutraceuticals. Molecules 21. 10.3390/molecules21111531.

Gautam, R., Kumar, N., Lynam, J.G., 2020. Theoretical and experimental study of choline chloride-carboxylic acid deep eutectic solvents and their hydrogen bonds. J. Mol. Struct. 1222, 128849 https://doi.org/10.1016/j.molstruc.2020.128849.

Göke, K., Lorenz, T., Repanas, A., Schneider, F., Steiner, D., Baumann, K., Bunjes, H., Dietzel, A., Finke, J.H., Glasmacher, B., Kwade, A., 2018. Novel strategies for the formulation and processing of poorly water-soluble drugs. Eur. J. Pharm. Biopharm. https://doi.org/10.1016/j.ejpb.2017.05.008.

Gutiérrez, A., Aparicio, S., Atilhan, M., 2019. Design of arginine-based therapeutic deep eutectic solvents as drug solubilization vehicles for active pharmaceutical ingredients. PCCP 21, 10621–10634. https://doi.org/10.1039/c9cp01408j.

Hansen, B.B., Spittle, S., Chen, B., Poe, D., Zhang, Y., Klein, J.M., Horton, A., Adhikari, L., Zelovich, T., Doherty, B.W., Gurkan, B., Maginn, E.J., Ragauskas, A., Dadmun, M., Zawodzinski, T.A., Baker, G.A., Tuckerman, M.E., Savinell, R.F., Sangoro, J.R., 2021. Deep eutectic solvents: a review of fundamentals and applications. Chem. Rev. 121, 1232–1285. https://doi.org/10.1021/acs.chemrev.0c00385.

Hasa, D., Schneider Rauber, G., Voinovich, D., Jones, W., 2015. Cocrystal formation through mechanochemistry: from neat and liquid-assisted grinding to polymer-assisted grinding. Angew. Chem. Int. Ed. 54, 7371–7375. https://doi.org/10.1002/anie.201501638.

Liu, Y., Friesen, J.B., McAlpine, J.B., Lankin, D.C., Chen, S.-N., Pauli, G.F., 2018. Natural deep eutectic solvents: properties, applications, and perspectives. J. Nat. Prod. 81, 679–690. https://doi.org/10.1021/acs.jnatprod.7b00945.

Liu, Y., Wu, Y., Liu, J., Wang, W., Yang, Q., Yang, G., 2022. Deep eutectic solvents: recent advances in fabrication approaches and pharmaceutical applications. Int. J. Pharm. 622, 121811 https://doi.org/10.1016/j.ijpharm.2022.121811.

Merisko-Liversidge, E., Liversidge, G.G., 2011. Nanosizing for oral and parenteral drug delivery: a perspective on formulating poorly-water soluble compounds using wet media milling technology. Adv. Drug Deliv. Rev. 63, 427–440. https://doi.org/10.1016/j.addr.2010.12.007.

Mišan, A., Nađpal, J., Stupar, A., Pojić, M., Mandić, A., Verpoorte, R., Choi, Y.H., 2020. The perspectives of natural deep eutectic solvents in agri-food sector. Crit. Rev. Food Sci. Nutr. https://doi.org/10.1080/10408398.2019.1650717.

Mokhtarpour, M., Shekaari, H., Zafarani-Moattar, M.T., Golgoun, S., 2020. Solubility and solvation behavior of some drugs in choline based deep eutectic solvents at different temperatures. J. Mol. Liq. 297, 111799 https://doi.org/10.1016/j.molliq.2019.111799.

Mustafa, N., Spelbos, V., Witkamp, G.-J., Verpoorte, R., Choi, Y., 2021. Solubility and stability of some pharmaceuticals in natural deep eutectic solvents-based formulations. Molecules 26, 2645. https://doi.org/10.3390/molecules26092645.

Olivares B, Martínez F, Rivas L, Calderón C.M, Munita J.R, Campodonico P., 2018. A Natural Deep Eutectic Solvent Formulated to Stabilize β-Lactam Antibiotics. Scientific Reports 8. 10.1038/s41598-018-33148-w.

Park H, Seo H.J, Ha E.S, Hong S. hyeon, Kim J.S, Kim M.S, Hwang S.J, 2020. Preparation and characterization of glimepiride eutectic mixture with L-arginine for improvement of dissolution rate. International Journal of Pharmaceutics 581, 119288. 10.1016/j.ijpharm.2020.119288.

Patel, V., Lalani, R., Bardoliwala, D., Ghosh, S., Misra, A., 2018. Lipid-Based Oral Formulation Strategies for Lipophilic Drugs. AAPS PharmSciTech 19, 3609–3630. https://doi.org/10.1208/s12249-018-1188-8.

Rozas, S., Benito, C., Alcalde, R., Atilhan, M., Aparicio, S., 2021. Insights on the water effect on deep eutectic solvents properties and structuring: The archetypical case of choline chloride + ethylene glycol. J. Mol. Liq. 344, 117717 https://doi.org/10.1016/j.molliq.2021.117717.

Savi, L.K., Dias, M.C.G.C., Carpine, D., Waszczynskyj, N., Ribani, R.H., Haminiuk, C.W.I., 2019. Natural deep eutectic solvents (NADES) based on citric acid and sucrose as a potential green technology: a comprehensive study of water inclusion and its effect on thermal, physical and rheological properties. Int. J. Food Sci. Technol. 54, 898–907. https://doi.org/10.1111/ijfs.14013.

Shafie, M.H., Yusof, R., Gan, C.-Y., 2019. Synthesis of citric acid monohydrate-choline chloride based deep eutectic solvents (DES) and characterization of their physicochemical properties. J. Mol. Liq. 288, 111081 https://doi.org/10.1016/j.molliq.2019.111081.

Smith, E.L., Abbott, A.P., Ryder, K.S., 2014. Deep Eutectic Solvents (DESs) and Their Applications. Chem. Rev. 114, 11060–11082. https://doi.org/10.1021/cr300162p.

Sut S, Faggian M, Baldan V, Poloniato G, Castagliuolo I, Grabnar I, Perissutti B, Brun P, Maggi F, Voinovich D, Peron G, Dall'Acqua S, 2017. Natural Deep Eutectic Solvents (NADES) to enhance berberine absorption: An in vivo pharmacokinetic study. Molecules 22. 10.3390/molecules22111921.

Wang, H., Liu, S., Zhao, Y., Wang, J., Yu, Z., 2019. Insights into the Hydrogen Bond Interactions in Deep Eutectic Solvents Composed of Choline Chloride and Polyols. ACS Sustain. Chem. Eng. 7, 7760–7767. https://doi.org/10.1021/acssuschemeng.8b06676.

Zahrina, I., Mulia, K., Yanuar, A., Nasikin, M., 2018. Molecular interactions in the betaine monohydrate-polyol deep eutectic solvents: Experimental and computational studies. J. Mol. Struct. 1158, 133–138. https://doi.org/10.1016/j.molstruc.2017.11.064.

Zainal-Abidin, M.H., Hayyan, M., Ngoh, G.C., Wong, W.F., Looi, C.Y., 2019. Emerging frontiers of deep eutectic solvents in drug discovery and drug delivery systems. J. Control. Release 316, 168–195. https://doi.org/10.1016/j.jconrel.2019.09.019.

Zanolla, D., Perissutti, B., Passerini, N., Chierotti, M.R., Hasa, D., Voinovich, D., Gigli, L., Demitri, N., Geremia, S., Keiser, J., Cerreia Vioglio, P., Albertini, B., 2018. A new soluble and bioactive polymorph of praziquantel. Eur. J. Pharm. Biopharm. 127, 19–28. https://doi.org/10.1016/j.ejpb.2018.01.018.

Zhao, B.-Y., Xu, P., Yang, F.-X., Wu, H., Zong, M.-H., Lou, W.-Y., 2015. Biocompatible Deep Eutectic Solvents Based on Choline Chloride. Characterization and Application to the Extraction of Rutin from *Sophora japonica*. ACS Sustain. Chem. Eng. 3, 2746–2755. https://doi.org/10.1021/acssuschemeng.5b00619.

Zhekenov, T., Toksanbayev, N., Kazakbayeva, Z., Shah, D., Mjalli, F.S., 2017. Formation of type III Deep Eutectic Solvents and effect of water on their intermolecular interactions. Fluid Phase Equilib. 441, 43–48. https://doi.org/10.1016/j.fluid.2017.01.022.